Direct Tests of a Pixelated Microchannel Plate as the Active Element of a Shower Maximum Detector

SURF Final Report

Federico Presutti
Mentor: Maria Spiropulu
Co-Mentor: Artur Apresyan, Si Xie, Cristian Pena

Abstract

One possibility to make a fast and radiation resistant shower maximum detector is to use a secondary emitter as an active element. We further the study of microchannel plate photomultipliers (MCPs) as the active element of a shower-maximum detector. We present test beam results obtained using Photonis XP85011 and Photek 240 MCPs to detect secondary particles of an electromagnetic shower. We focus on the use of the multiple pixels on the Photonis MCP in order to find a transverse two-dimensional shower maxima distribution. A submillimeter spatial resolution of 0.6 mm and 0.9 mm (x and y axes respectively) was obtained with an 8 GeV electron beam. A method for measuring time resolution from the Photonis MCP as a whole is presented, and it improves the time resolution for individual pixel readouts. The time resolution is found to be better than 40 ps.

Introduction

Future high-energy physics experiments can benefit substantially from shower-maximum detectors or calorimeters with improved timing capability.

Past studies have indicated that using microchannel plates (MCP) as the active element of a shower-maximum detector or a calorimeter is a promising option for achieving time measurement precision at the level of a few tens of picoseconds [1, 2, 3]. Moreover, such devices are intrinsically radiation hard and thus would tolerate the harsh radiation environment at future hadron colliders. A further advantage of MCP's is their capability for pixelated readout, allowing for the possibility of a highly granular calorimeter with sub-millimeter spatial resolution, allowing for substantial improvement in physics at the TeV scale.

We report on the first studies of a high-granularity shower-maximum detector that uses the Photonis XP85011 MCP as the active element to detect direct secondary emission particles. The MCP is used to sample the electromagnetic shower induced by a beam of electrons impacting a tungsten absorber layer that has a thickness of about 4 radiation lengths. The active area of the MCP-PMT is pixelated, with square pixels of size 6 mm, and individual pixels are read out through separate electronic channels. The energy of the electromagnetic showers is reconstructed using the total collected charge and the positions are reconstructed using a simple energy-weighting algorithm. Through the use of a high-precision motorized stage, a position scan is performed during beam-tests and the position resolution of the shower-maximum detector is obtained. Finally, we investigate various timing properties of such a pixelated shower-maximum detector.

Experimental Setup

The experiment was performed at the MTEST location of the Fermilab Test Beam Facility using

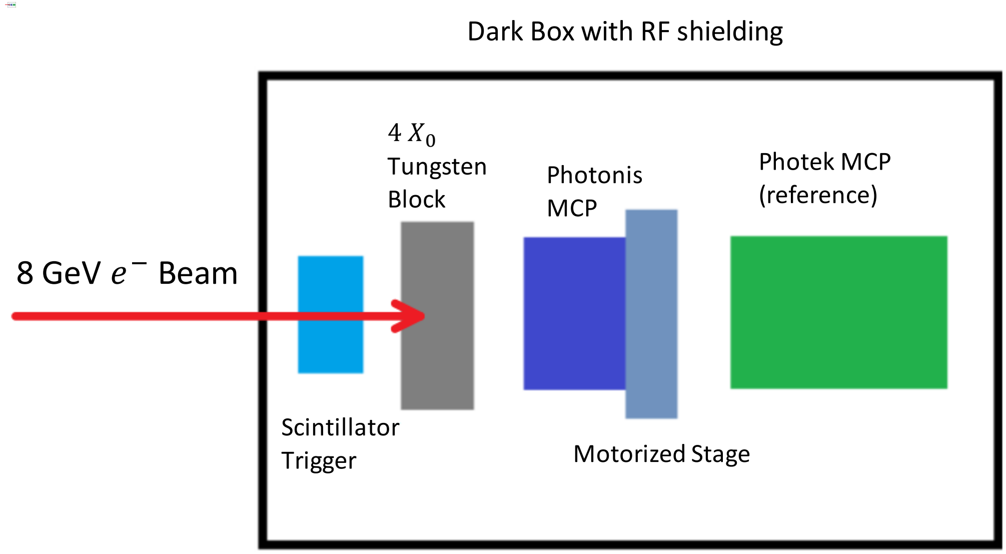

Figure 1: A diagram of the experimental setup is shown. An electron beam is directed towards a tungsten block within the dark box, where an electromagnetic shower incident on the MCPs is created.

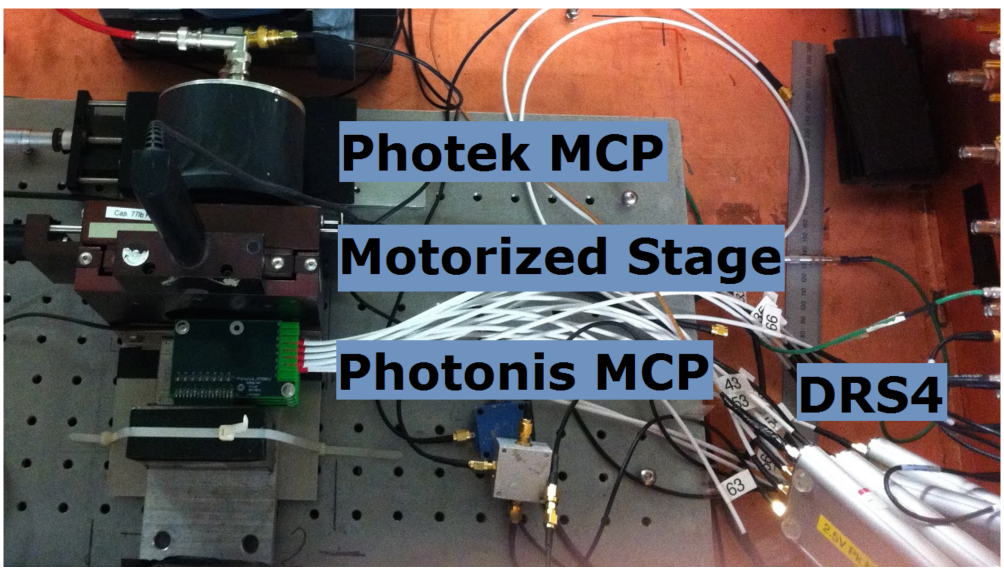

Figure 2: The experimental setup inside of the dark box is shown. The beam direction is from the bottom of the photograph to the top. The detector elements shown in the order from upstream to downstream of the beam are: the tungsten absorber, the Photonis XP85011 MCP located on the on the motorized stage, and the Photek 240 MCP used as a time reference detector. The DRS4 waveform digitizers are also shown on the lower right side.

an 8 GeV electron beam. A differential Cherenkov counter, located upstream of the setup, was used to select for electron events (and ignore possible pion or other particle events). All other detectors were placed inside a dark box lined with copper foil for electromagnetic shielding. A diagram of the experimental setup is shown in Figure 2, and photograph of the setup within the dark box is shown in Figure 2.

A scintillator of size 1.7 mm× 2.0 mm was used to trigger the data acquisition and to constrain the trajectory of the electrons from the beam. Downstream of the trigger, was a tungsten absorber with a thickness of about 1 cm, equivalent to about 4 radiation lengths (X_0). The Photonis XP85011 MCP with pixelated readout was set on a high precision motorized stage and placed behind this absorber. A Photek 240 MCP-PMT, whose time resolution was previously measured to be less than 10 ps [3], was used to record the reference time-stamp, placed behind the first MCP to avoid that the incoming electrons interact and shower on it instead of the absorber. Four DRS4 high speed waveform digitizers were used to acquire the signals from the various MCP channels and the differential Cherenkov counter.

A picture of the Photonis XP85011 MCP and a schematic diagram are shown in Figure 3. The MCP has a a total of 64 pixels arranged in an 8×8 square that can be read out individually. The nine pixels shown within the red square were used. During the course of the experiment we found that one pixel (labeled 44 in Figure 3) did not function properly and was therefore ignored in the analysis of the data.

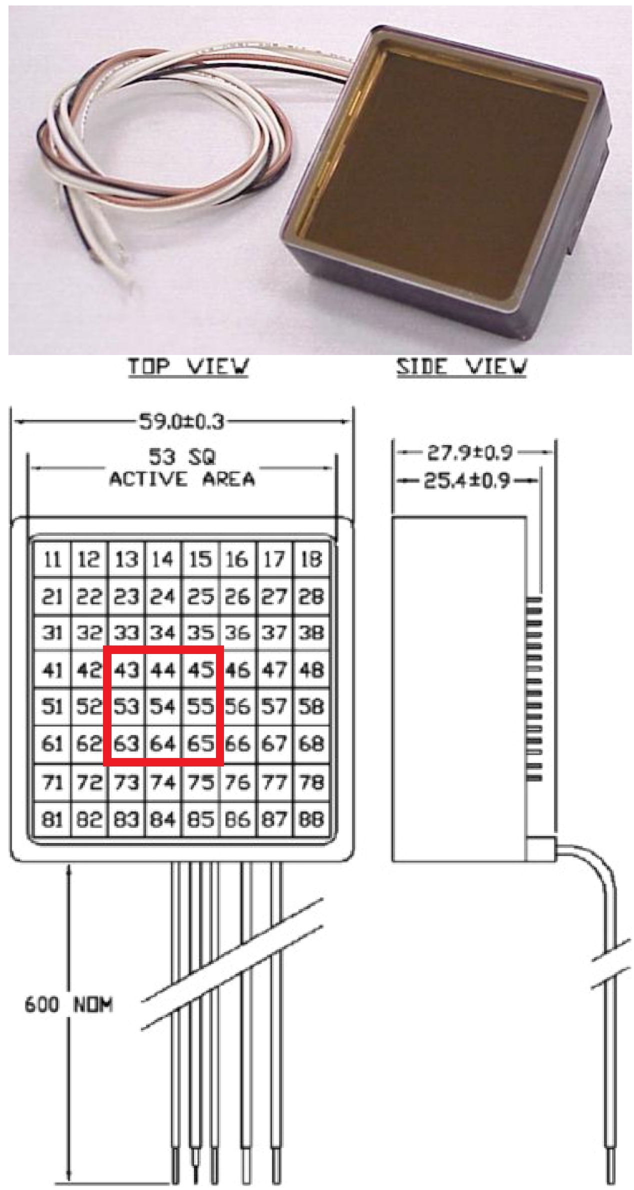

Figure 3: The external view of the Photonis XP85011 MCP is shown on top, and the schematic diagram is shown below it. The red square indicates the pixels used for the experiment and data analysis.

Electromagnetic Shower Maximum Position

Figure 4 has example pulses from one pixel channel of the Photonis XP85011 MCP and the Photek 240 MCP-PMT digitized by the DRS4.

The energy deposited on each pixel is proportional to the number of secondary particles from the electromagnetic shower incident of the MCP device, which is in turn proportional to the cumulative charge of the incident particles. The charge is computed by summing the nine voltage sample around the peak of the pulse, and scaling by the 50 Ω impedance of the setup. The sampling period is approximately 0.2 ns. Events containing pulses above 500 mV in amplitude are rejected as they saturate the DRS4, and pulses with amplitude lesser than 20 mV are ignored, to reduce the impact of electronic noise. Other event selection and pulse cleaning criteria are used to eliminate abnormal pulses in the readout.

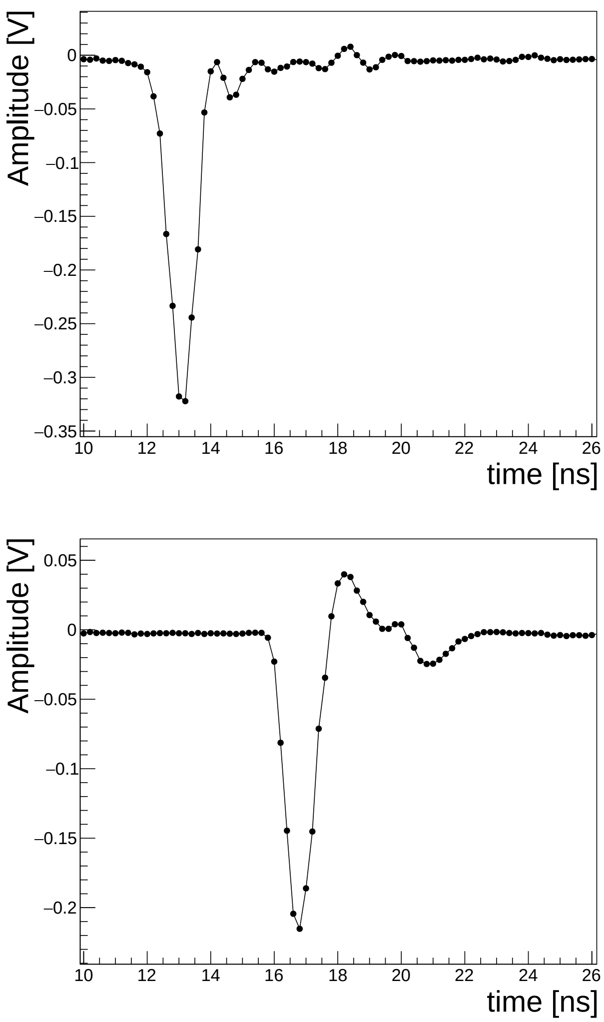

Figure 4: Example of a signal from a single Photonis pixel (top) and Photek (bottom) MCP following a high-energy electron shower, digitized with a DRS4.

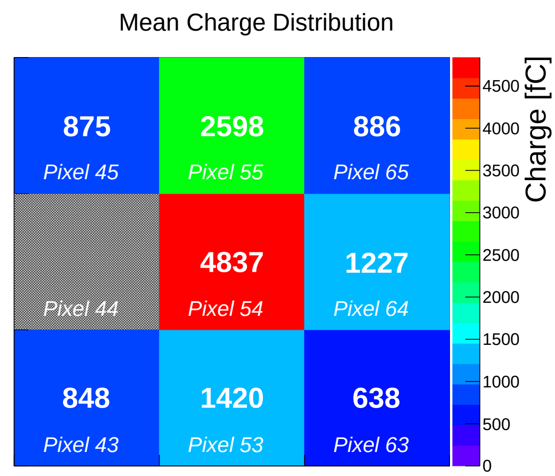

Figure 5: The mean charge measured for each pixel for one example run is shown. During this run, the Photonis MCP was held in the same location. Based on the distribution of the mean charge among the pixels, we can infer that the beam center is located in the upper half of the center pixel. Pixel 44 was found to be non-operational.

The transverse shape of electromagnetic showers is well understood and has a characteristic width given by the Moliere radius. For tungsten, the Moliere radius is about 9 mm. Therefore we expect the shower to be contained within two of the pixels in the Photonis XP85011 MCP, which has 6 mm sized pixels. Figure 5 shows the mean charge measured in each of the pixels for one example run where the beam was approximately centered on the Photonis MCP. The electron beam has a width of about 1 cm.

Each electron impact that induces an electromagnetic shower is defined as an event. For all events, the center position, $\vec{\mathbf{p}}$ of the electromagnetic shower is calculated based on the distribution of charge or energy (which are proportional quantities). This is done by weighing the pixel positions by the corresponding integrated charge as follows:

$$\vec{\mathbf{p}} = \frac{\sum_{i \in \text{pixels}} Q_i \vec{p}_i}{\sum_{i \in \text{pixels}} Q_i}$$

where i enumerates the individual pixels, Q_i is the charge collected in pixel i, and $\vec{p}_i$ is the vector describing the x and y coordinates of the center of pixel i. The origin of the coordinate system is chosen to be at the lower left corner of the 3×3 array of pixels.

Multiple runs were taken scanning different beam positions relative to the Photonis MCP by moving the motorized stage. Figure 6 demonstrates the distributions of the reconstructed shower positions for three example runs in which the beam was located near the top, center, and bottom of the center pixel. The fourth plot represents the projection of these distributions onto the y axis of the three runs together. The measured shower-maximum is observed to move consistent with the known movement of the motorized stage.

Electromagnetic Shower Maximum Spatial Resolution

For each run the center of the shower-maximum/beam-spot is determined by fitting the measured x and y coordinates with a Gaussian function and finding a mean for each dimension. The data from all runs are then combined by subtracting the x and y coordinates by their corresponding mean. This procedure is intended to center all events from all runs around the origin, in one large data set (see Fig 7).

The distribution of measured coordinates is modeled as a convolution of a flat distribution with width equal to the measured dimensions of the scintillator trigger, and a Gaussian resolution function. The spatial distribution of particles is unknown but is constrained to the area in the x-y plane covered by the scintillator in order to trigger an event, hence the assumption of a flat distribution. The Gaussian error function is on the assumption that the device measurements should have a normal error distribution when measuring identical events. Mathematically this is the convolution of a one-dimensional box function (the combination of two Heaviside θ functions) and a Gaussian function. The result is shown below (A and A' are proportionality constants that will depend on the sample number).

$$\begin{aligned} f(x) &= A\left[(\theta(x+a/2) - \theta(x-a/2)) * \exp\left(\frac{-(x-\mu)^2}{2\sigma^2}\right)\right] \\ &= A'\left[\operatorname{erf}\left(\frac{2x-2\mu+a}{2\sqrt{2}\sigma}\right) + \operatorname{erf}\left(\frac{2\mu-2x+a}{2\sqrt{2}\sigma}\right)\right] \end{aligned}$$

A maximum likelihood fit is performed on the data using this model. Using a fixed a to 1.7 mm for the x axis and 2.0 mm for the y axis. The position resolution of the detector is measured as the width of the gaussian resolution function. We measure the resolution as 0.55 ± 0.2 mm and 0.91 ± 0.2 mm for x and y respectively, with an additional systematic uncertainty of 0.15mm due to the uncertainty in the exact beam-spot shape.

Electromagnetic Shower Time Resolution

Gaussian fits to the peak region of the signal-pulse, such as those in Figure 4, are used to reconstruct the time-stamps for each pixel in each event. We reconstruct the time-stamp t of the entire electromagnetic shower by considering all the pixels and using the same energy weighting procedure that was used above for the shower position reconstruction:

$$t = \frac{\sum_{i \in \text{pixels}} Q_i t_i}{\sum_{i \in \text{pixels} Q_i}}$$

where i labels the individual pixels, Q_i is the charge collected in pixel i, and t_i is the reconstructed time-stamp for pixel i. Alternatively, the more naive algorithm that uses the time-stamp from the one pixel with the highest energy/charge deposit, was also studied. Figure 8 shows example time-stamp distributions for these two methods of shower time reconstruction on the same run.

Figure 9, compares the time resolution for electromagnetic showers computed using the two methods described above for all runs. The time resolution for the pixel with the largest energy deposit is around 70 ps and 85 ps, depending on the run. Using the energy weighted algorithm improves the time resolution consistently to about 50 ps.

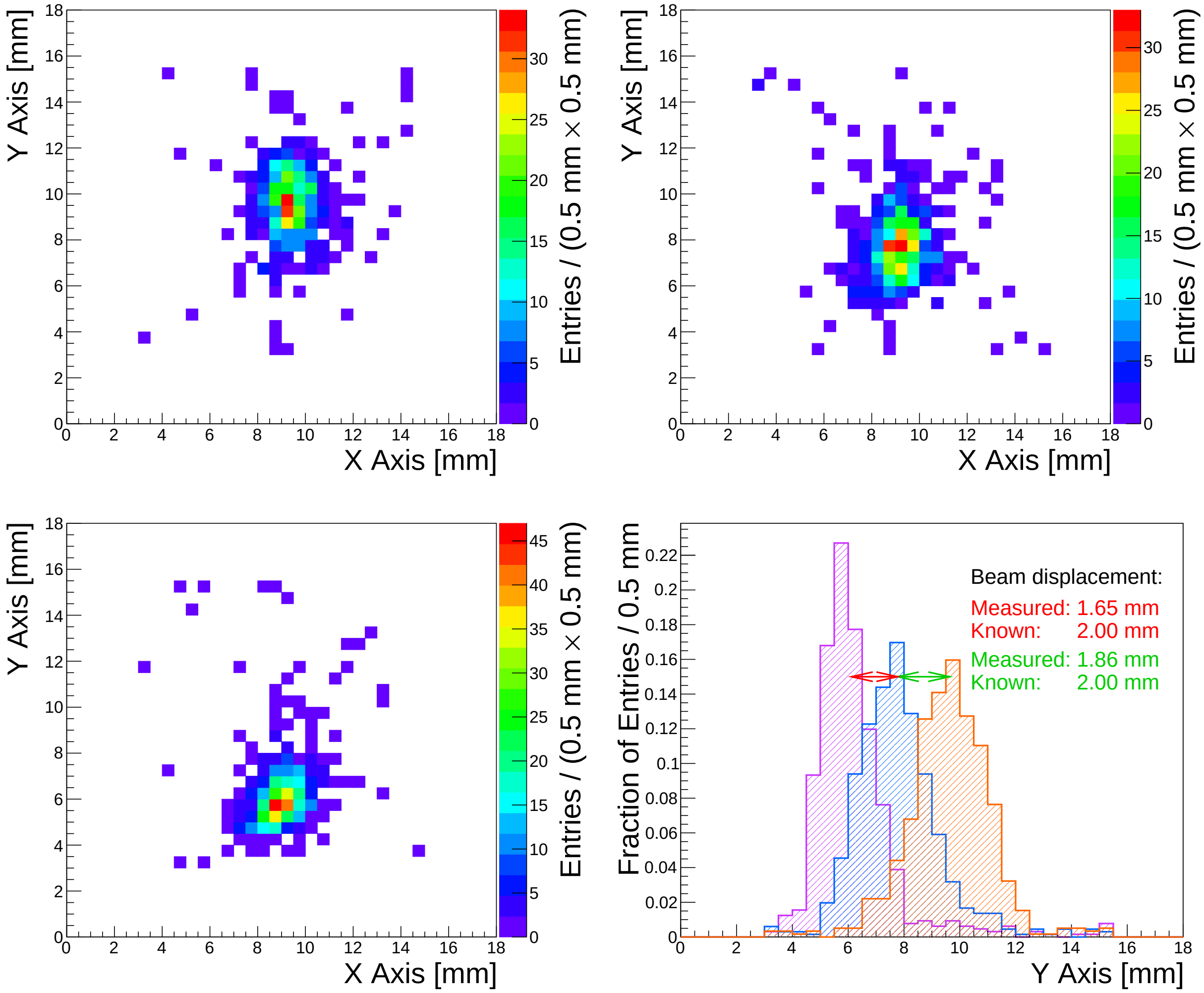

Figure 6: The distribution of reconstructed shower positions is shown for three runs with the beam centered near the top, center, and bottom of the central pixel. The last plot represents the projections onto the y axis to demonstrate the movement of the shower-maximum between runs.

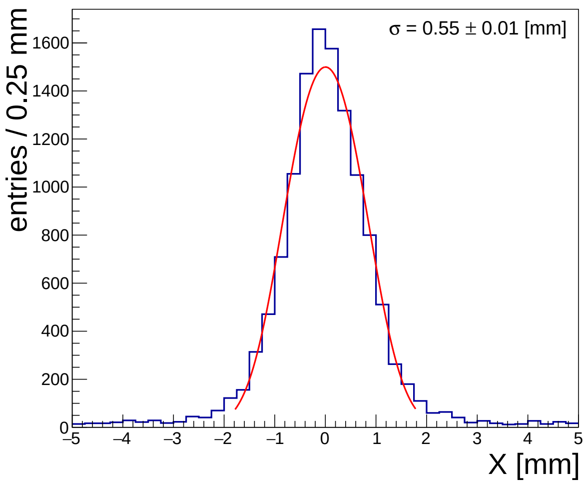

Figure 7: The distributions of the measured x (left) and y (right) coordinates are shown along with the fit to the resolution model. The position resolution of the EM shower as measured by the MCP detector is determined from the fit to the resolution model.

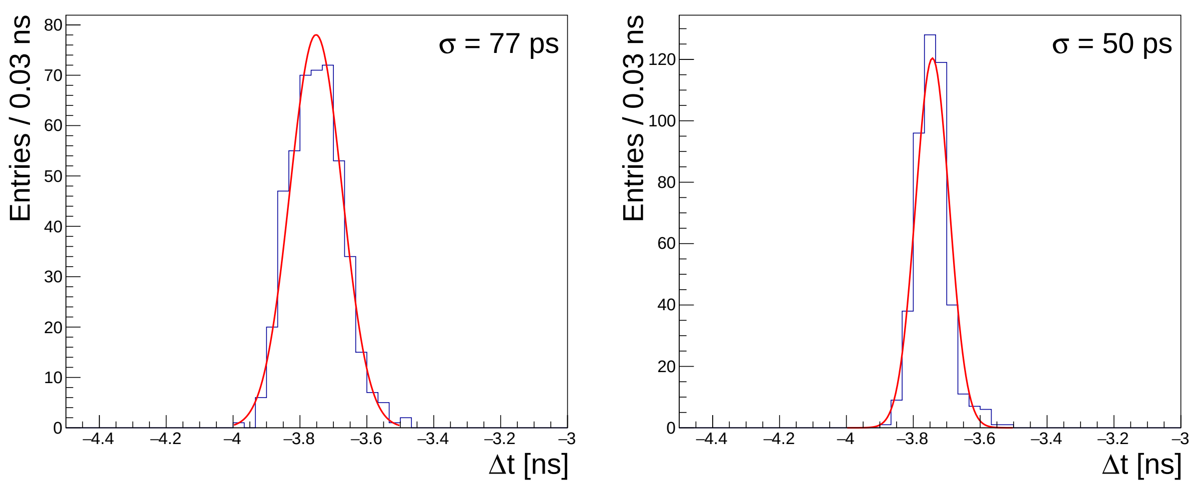

Figure 8: The time distributions obtained using the highest energy pixel (left) and the energy weighted algorithm (right) are shown for one example run. The distributions are fitted with Gaussian models, and the width parameter of the Gaussian is displayed on the plot.

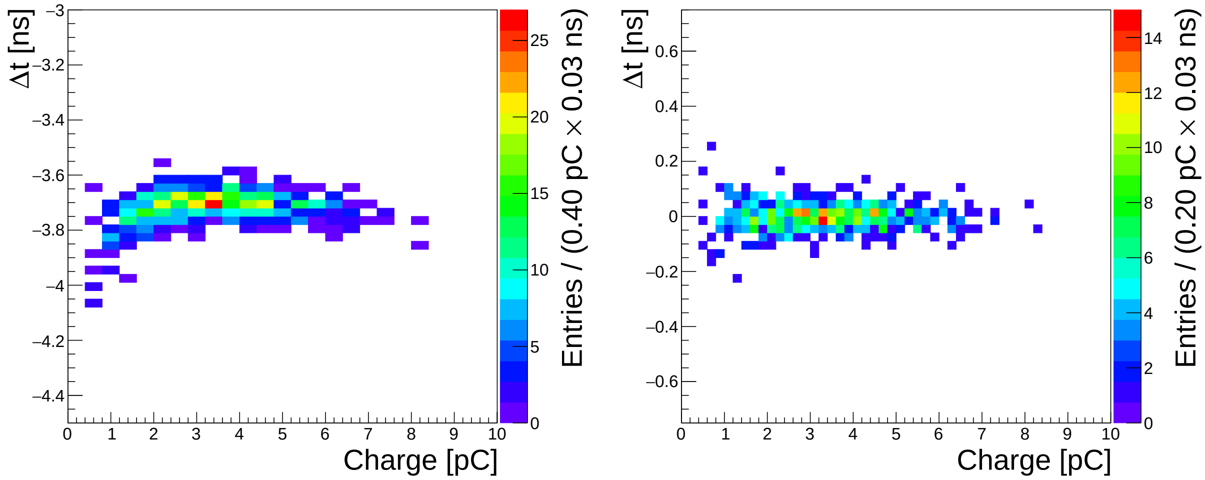

Figure 10: The correlation between the time measurement and the measured integrated charge is shown on the left for one example pixel. The same correlation after performing the time measurement correction is shown on the right.

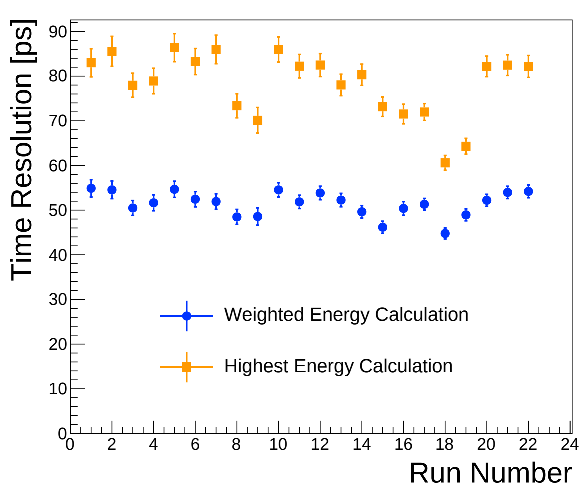

Figure 9: Time resolution found for each run. The time-stamp weighting method consistently results in under 60 ps. Notice how the highest-signal-pixel method for picking the time-stamp value is significantly worse.

We found that the time measurements made using the Photonis MCP exhibit a dependence on the pulse amplitude or integrated charge. This dependence is shown in Figure 10, and is observed to be approximately the same for all pixels. A correction was performed to the in order to flatten the dependence of the time measurement on the integrated charge as shown on the right panel of Figure 10. After performing this time measurement correction, the time resolution measurements improve to about 35 ps and is shown in Figure 11.

Finally, we studied the dependence of the electromagnetic shower time resolution as a function of the maximum number of pixels included in the energy-weighted algorithm. Figure 12 shows this dependence for one example run. The time resolution improves according to a $1/\sqrt{N}$ scaling up to about 3 or 4 pixels, but then generally flattens, or sometimes even slightly worsens, with the inclusion of more pixels. The initial $1/\sqrt{N}$ scaling is encouraging as it indicates that further granularity (smaller pixel size) should improve the time resolution. It is to be expected that the curve flattens out with the inclusion of more pixels since most of the shower is con-

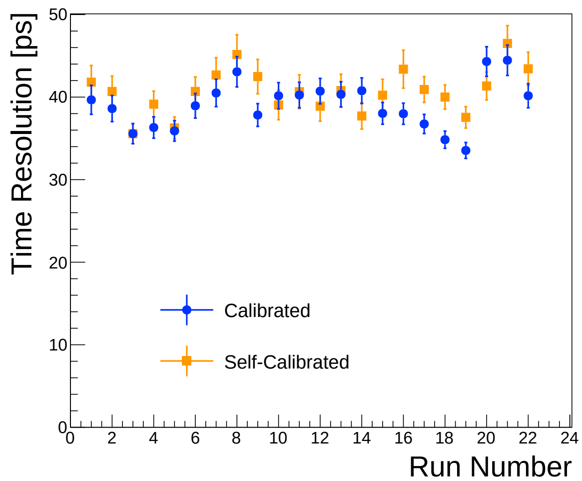

Figure 11: The time resolution of the electromagnetic shower for various runs is shown after performing the time measurement correction based on the measured integrated charge.

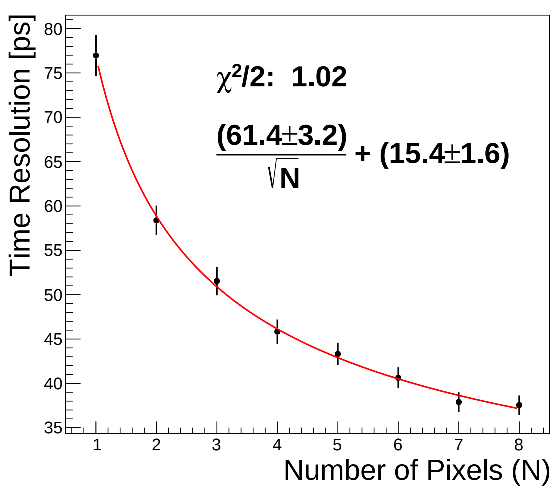

Figure 12: The time resolution is plotted as a function of the number of pixels included in the energy-weighted algorithm for one example run.

tained within the few pixels closest to the center of the shower, and additional pixels do not provide additional information.

Summary of Results

A high-granularity shower-maximum detector that uses an MCP as an active element has been studied. We found that this detector prototype has a submillimeter spatial resolution. Using the simple algorithm presented, based on the electromagnetic shower's charge deposit on each pixel, we obtained a resolution of 0.55 ± 0.01 mm in the x axis, and 0.91 ± 0.01 mm in the y axis, where the MCP pixel size was 6 mm for both axes. It is unclear as of yet why the x and y resolutions do not closely match; it may have to do with the asymmetry introduced by the MCP's non-operational pixel. The time resolution obtained was better than 40 ps following calibrations and using the algorithm proposed. We also found that time resolution improved by a rate of $1/\sqrt{N}$ suggesting that higher granularity could improve resolution.

Acknowledgements

I would like to thank my mentors Maria Spiropulu, Artur Apresyan, Si Xie and Cristian Pena for this opportunity to participate in this project and for their help and support.

References

[1] A. Ronzhin, S. Los, E. Ramberg, *et al.*, "Development of a new fast shower maximum detector based on microchannel plates photomultipliers (MCP-PMT) as an active element," *NIM* **A** *759 (2014) 65-73.*

[2] A. Ronzhin, S. Los, E. Ramberg, A. Apresyan, S. Xie, M. Spiropulu, and H. Kim, "Direct tests of micro channel plates as the active element of a new shower maximum detector," *Nucl. Instrum. Meth.*, vol. A795, pp. 52–57, 2015.

[3] A. Ronzhin, S. Los, E. Ramberg, A. Apresyan, S. Xie, M. Spiropulu, and H. Kim, "Direct tests of micro channel plates as the active element of a

new shower maximum detector," *Nucl. Instrum. Meth.*, vol. A795, pp. 288–292, 2015.